# High-Frequency Polymer Modulators with Integrated Finline Transitions and Low $V_\pi$

Datong Chen, Daipayan Bhattacharya, Anand Udupa, Boris Tsap, Harold R. Fetterman, *Fellow, IEEE,* Antao Chen, Sang-Shin Lee, Jinghong Chen, William H. Steier, *Fellow, IEEE,* and Larry R. Dalton

***Abstract*— Ultrahigh-speed integrated electrooptic polymer phase modulators have been fabricated and tested. They are made from a new nonlinear optical polymer, amino phenylene isophorone isoxazolone (APII), and are incorporated with integrated high-speed electrode transitions for $W$-band (75–110 GHz) operation. This new polymer has also been used to fabricate Mach–Zehnder modulators. These devices show good performance over a wide frequency band ranging to 40 GHz and have a $V\pi < 10$ V. The measurements establish APII, and other chromophores specially designed to minimize chromophore–chromophore interaction, as strong contenders for fabricating modulators for commercial and military applications.**

***Index Terms*—Electrooptic modulation, finline transition, optical mixing, optical waveguides, traveling-wave devices.**

NONLINEAR optical polymer materials have become a viable option for future high-performance integrated optics. This is especially true for high-frequency optical circuits because of their high nonlinearity, fast electronic response and near ideal velocity match for traveling-wave devices. Recent progress in research on nonlinear optical polymer materials and devices made from them confirm these predictions [1]–[4].

Previously, we demonstrated the operation of polymer traveling-wave phase modulators up to 110 GHz [5]. In those experiments, we used commercial coplanar waveguide probes (Picoprobe Model 120) to launch the driving power into the modulators. Though these probes provided excellent coupling of the power up to 120 GHz, they are unsuitable for integrated modulator structures due to their cost, size, and geometry. In this paper, we present the design and fabrication of a set of devices with monolithically integrated antipodal finline transitions, the structure of which is shown in Fig. 1. It has the advantage of low loss and high-dimensional fabrication tolerance. The transition gradually transforms the electric field

Manuscript received August 3, 1998; revised September 15, 1998. This work was supported by the Air Force Office of Scientific Research and by the Office of Naval Research.

D. Chen was with the Department of Electrical Engineering, University of California, Los Angeles, CA 90095 USA. He is now with Hewlett-Packard Laboratory, Palo Alto, CA 94304 USA.

D. Bhattacharya, A. Udupa, and H. R. Fetterman are with the Department of Electrical Engineering, University of California, Los Angeles, CA 90095 USA.

B. Tsap was with the Department of Electrical Engineering, University of California, Los Angeles, CA 90095 USA. He is now with Pacific Wave Industries, Los Angeles, CA 90024 USA.

A. Chen, S.-S. Lee, J. Chen, W. H. Steier, and L. R. Dalton are with the Department of Electrical Engineering and Chemistry, University of Southern California, Los Angeles, CA 90089 USA.

Publisher Item Identifier S 1041-1135(99)00339-0.

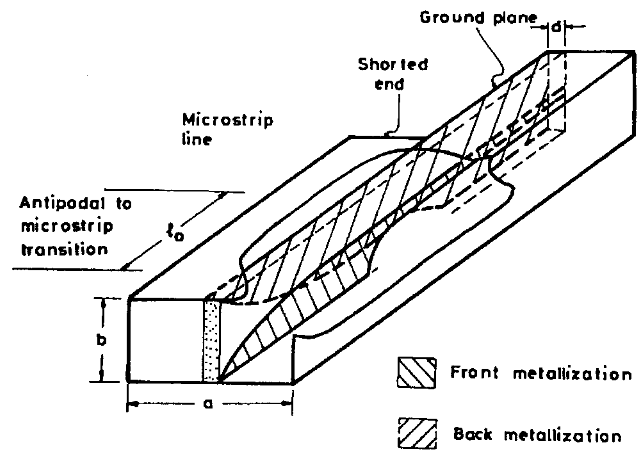


(a)

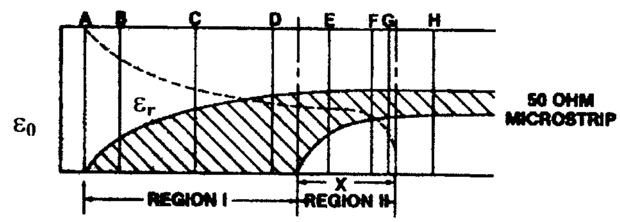


(b)

Fig. 1. (a) Design of the finline transition. (b) The changing overlap between the top and bottom electrodes gradually rotates the electric field by 90°.

profile of the rectangular metallic waveguide to that of the microstrip line electrode on the device and effectively couples the microwave driving power into the modulator.

We chose to use a 127-$\mu$m-thick Mylar film as the dielectric substrate owing to its low microwave loss tangent; good electrical, chemical, thermal and mechanical properties. The Mylar film was glued onto a silicon wafer for mechanical support during processing and detached from it just before insertion into the waveguide. A layer of silver and gold was deposited on the Mylar to serve as the lower ground plane for the microstrip lines.

Using photolithography, the lower finline transition pattern was etched in the region to be inserted into the waveguide. The lower cladding layer and the active polymer layer were spin coated and the active polymer was corona poled. The optical waveguide pattern was defined on the polymer using reactive ion etching with alignment to the pre-etched ground pattern. The upper cladding was spun on and a thin layer of chromium and gold was deposited for the top electrode.

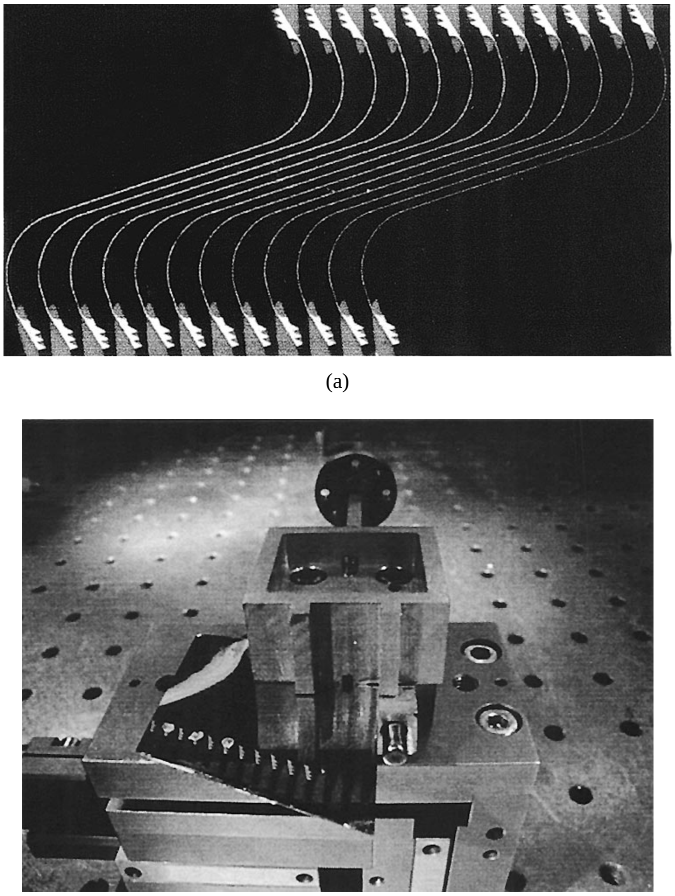

(a)

(b)

Fig. 2. (a) Photograph of the fabricated polymer modulator with integrated finline transitions at both ends of the traveling-wave electrode. (b) Photograph of the packaged $W$-band polymer modulator. This shows one modulator in the array connected to the rectangular waveguide.

A thick photoresist was patterned to define the top electrode and the upper finline transition. This pattern was precisely aligned to the polymer optical waveguide and the lower finline. Electrochemical gold plating was used to increase the thickness of the top electrode to 7 $\mu$m. The end surfaces of the optical waveguide were prepared using a dicing saw. A photograph of the fabricated device is shown in Fig. 2(a). The particular finline transition region to be inserted into the rectangular waveguide was separated from the array and the polymer layers on the lower finline transition pattern removed using a solvent. The transition was then inserted into the waveguide as shown in Fig. 2(b).

Previously, we have made polymer modulator devices using PUR-DR 19 that had an electrooptic coefficient $r_{33} = 15$ pm/V, about half that of $LiNbO_3$. Recent efforts in nonlinear organic chemistry have resulted in the synthesis of polymers with electrooptic coefficients close to or even exceeding that of $LiNbO_3$. This is a direct consequence arising out of a better understanding of the London forces governing the dipole–dipole electrostatic interactions [6]. One such polymer developed by Dalton *et al.* is amino phenylene isophorone isoxazolone (APII) which has a $r_{33} = 30$ pm/V at an optical wavelength of 1.06 $\mu$m [1]. In addition to impressive nonlinearities, APII has exhibited low optical losses and high stability. Fig. 3 shows the intrinsic optical loss ($\sim$1 dB/cm) of the APII as a function of the propagating distance of light. The temporal stability of the induced acentric dipole alignment is achieved by incorporating chromophores into a crosslinked polyurethane thermosetting network. This increases the optical losses slightly, but makes these systems very robust. We have used them with relatively high-power levels (>20 mW) for long periods of time. APII exhibits high thermal stability, the decomposition temperature being 235 °C. Alignment temporal stability ranges from 90 °C to 120 °C for a crosslinked polymer network.

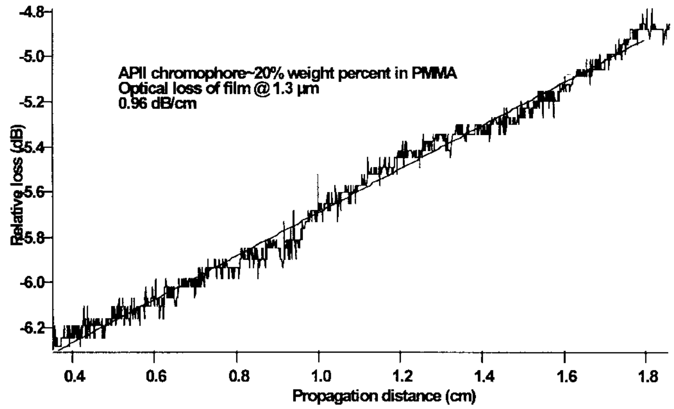


Fig. 3. Optical loss of the APII as a function of the propagating distance. Note that losses typically increase after crosslinking.

The performance of these APII polymer devices was measured using an optical heterodyne technique [7]. This technique involves mixing of the modulated output of our device and the output of a tunable laser that is set at a fixed frequency away from the center frequency of the modulated laser beam. A generalized schematic of this measurement is shown in Fig. 4(a). Assuming small-signal case, one of the terms generated by the beating between the three arms has a frequency $\Delta f = f - (F_1 - F_2)$ and has the following form:

$$E_1 E_3 \cdot \frac{\pi V_m}{V_\pi} \cdot \sin[2\pi \cdot \Delta f \cdot t - \Delta\phi] \quad (1)$$

where $E_1$ and $E_3$ are electric field strengths in the first and third arm, respectively, $V_m$ and $f$ are the peak voltage and frequency of the microwave signal, $F_1 - F_2$ and $\Delta\phi = \phi_1 - \phi_3$ are the difference in frequency and static phase between the two lasers and $V_\pi$ is the half-wave voltage of the phase modulator. By tuning the two lasers, $\Delta f$ can be made to fall in the IF band of our detection setup. The magnitude of the photocurrent generated by the detector is inversely proportional to the $V_\pi$ of the modulator at the frequency of operation. Since it depends only on the interaction between the phase-modulated arm and the heterodyne arm, this technique can be used equivalently to measure the frequency performance of phase and Mach–Zehnder modulators.

Light from a diode-pumped Nd:YAG laser ($\lambda = 1310$ nm) was butt-coupled to the optical waveguide endface of our modulator using a single-mode PM fiber. Light for the local oscillator was derived from an external-cavity semiconductor diode laser, which could be tuned several hundreds of gigahertz around the Nd:YAG laser. Fine tuning of the difference frequency was achieved by precisely adjusting the frequency

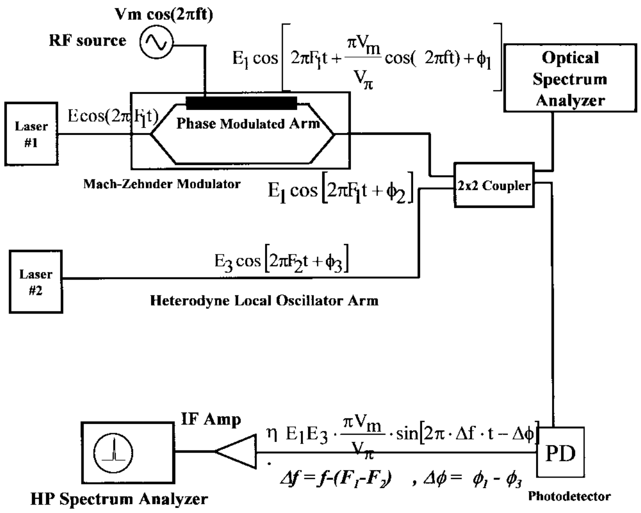


(a)

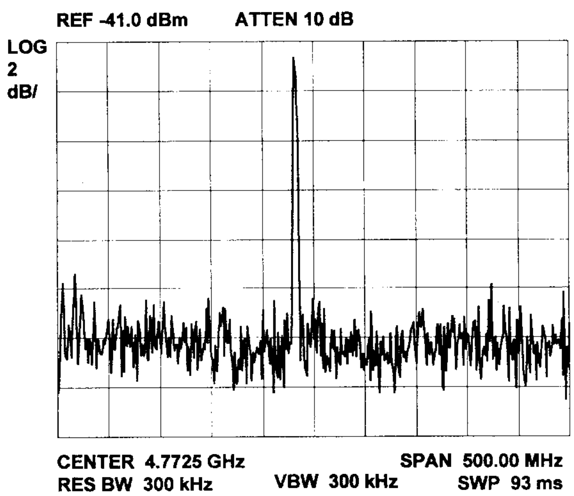


(b)

Fig. 4. (a) Generalized schematic of the optical heterodyne setup showing the Mach–Zehnder structure and local oscillator configuration. (b) Modulation signal of the APII phase modulator at 95 GHz down-converted to an IF of 4.77 GHz.

of the Nd:YAG laser. Both beams were combined using a $2 \times 2$ fiber beam splitter and made incident on a photodetector. A 50-mW GUNN diode was used as the microwave source at 95 GHz. The spectrum analyzer trace of the downconverted signal at 95 GHz for the APII integrated phase modulator is shown in Fig. 4(b). This is an encouraging result for a phase modulator that has a $V_\pi = 16$ V, that corresponds to a $V_\pi$ of 10.6 and 5.3 V in Mach–Zehnder and push–pull configurations, respectively.

To test the performance of the APII based modulators to 40 GHz, we fabricated a set of Mach–Zehnder devices on silicon substrates. The major fabrication steps were similar to those outlined for the devices on Mylar substrates. For an electrode–waveguide interaction length of 1.7 cm, the $V_\pi$ of these devices in a Mach–Zehnder configuration was 10 V. In a push–pull configuration, this would correspond to a $V_\pi = 5$ V, which makes this new set of polymer devices acceptable for commercial applications. Two tunable diode pumped Nd : YAG lasers at 1.319 $\mu$m were used as sources for lower frequency optical heterodyne measurement of the modulation signal. The initial measurements on the modulator showed considerable rolloff over the 0–40-GHz band of operation resulting from losses in the microstrip line. As we have found in related polymer structures, the $V_\pi$ can be made almost flat over this frequency range by increasing the thickness of the microstrip line.

Traditionally, it has been accepted that the main advantage of polymer modulators over $LiNbO_3$ modulators is their ultrahigh-theoretical bandwidth. This results from the polymers' almost perfect velocity match that allows them to be configured as traveling-wave devices [8]. However, the problem of the limited nonlinearities in polymer materials has so far kept them from finding widespread use. This new generation of polymer devices have shown vast improvement in performance over DR19 [9] and can compete with $LiNbO_3$ devices in many important applications.

In conclusion, APII, a new polymer material with high nonlinearity and low optical loss has been synthesized and used to fabricate arrays of ultrahigh-frequency phase modulators with integrated finline transitions. These modulators have been tested at 95 GHz. The excellent microwave performance of the integrated transition signals the first successful efforts in packaging of polymer modulators at such high frequencies. Using this new polymer, Mach–Zehnder modulators have been fabricated and shown to work over a wide frequency band. Both these devices have shown very low $V_\pi$ and have the ability to be commercially fabricated and packaged. Hence, these devices have widespread potential applications in commercial communication and military systems.

## REFERENCES

[1] J. Chen, J. Zhu, A. Harper, F. Wang, M. He, S. Mao, and L. R. Dalton, "Synthesis and characterization of a high-$\mu\beta$ chromophore containing the isophorone moiety for electro-optic applications," *Polymer Preprints*, vol. 38, no. 2, pp. 215–216, 1997.

[2] K. W. Beeson, P. M. Ferm, K. A. Horn, C. W. Knapp, M. J. McFarland, A. Nahata, J. Shan, C. Wu, and J. T. Yardley, "Polymeric electro-optic materials and devices: Meeting the challenges of practical applications," *Nonlinear Optical Properties of Organic Materials VI, Proc. SPIE*, 1993, vol. 2025, pp. 488–498.

[3] *Polymers for Second-Order Nonlinear Optics*, G. A. Lindsay and K. D. Singer, Eds. Washington DC: Amer. Chem. Soc., 1994.

[4] Y. Shi, W. H. Steier, L. Yu, M. Chen, and L. R. Dalton, "Large stable photoinduced refractive index change in a nonlinear optical polyester polymer with disperse red side groups," *Appl. Phys. Lett.*, vol. 58, no. 11, pp. 1131–1133, Mar. 1991.

[5] D. Chen, H. R. Fetterman, A. Chen, W. H. Steier, L. R. Dalton, W. Wang, and Y. Shi, "Demonstration of 110 GHz electro-optic polymer modulators," *Appl. Phys. Lett.*, vol. 70, no. 25, pp. 3335–3337, June 1997.

[6] L. R. Dalton, A. W. Harper, and B. H. Robinson, "The role of London forces in defining noncentrosymmetric order of high dipole moment-high hyperpolarizability chromophores in electrically poled polymeric thin films," *Proc. Nat. Acad. Sci. USA*, vol. 94, pp. 4842–4847, May 1997.

[7] W. Wang, D. Chen, H. R. Fetterman, Y. Shi, W. H. Steier, and L. R. Dalton, "Optical heterodyne detection of 60 GHz electro-optic modulation from polymer waveguide modulators," *Appl. Phys. Lett.*, vol. 67, no. 13, pp. 1806–1808, Sept. 1995.

[8] R. Lytel, "Applications of electro-optic polymers to integrated optics," in *Nonlinear Optical Materials and Devices for Photonic Switching, Proc. SPIE*, Jan. 1990, vol. 1216, pp. 30–40.

[9] W. Wang, D. Chen, H. R. Fetterman, Y. Shi, W. H. Steier, and L. R. Dalton, "Traveling wave electro-optic phase modulator using cross-linked nonlinear optical polymer," *Appl. Phys. Lett.*, vol. 65, no. 8, pp. 929–931, Aug. 1994.